AKADÉMIAI KIADÓ

The finite element modeling of rigid inclusion-supported embankment

Rashad Alsirawan* and Edina Koch

Department of Structural and Geotechnical Engineering, Széchenyi István University, H-9026, Győr, Hungary

Pollack Periodica • An International Journal for Engineering and Information Sciences

17 (2022) 2, 86–91

DOI:
10.1556/606.2021.00504

ORIGINAL RESEARCH PAPER

Received: April 20, 2021 • Revised manuscript received: November 28, 2021 • Accepted: December 13, 2021
Published online: May 26, 2022

ABSTRACT

The design of supported embankments on soft soil is a common challenge for civil engineers. This article aims to evaluate the performance of three advanced constitutive models for predicting the behavior of soft soils, i.e., hardening soil, hardening soil model with small-strain stiffness, and soft soil creep. A case study of a rigid inclusion-supported embankment is used for this purpose. Plaxis 3D program was adopted to predict the settlements in subsoil layers and vertical stresses in the load transfer platform. Comparison between field measurements and result of Plaxis 3D modeling was performed. Results demonstrate that soft soil creep model yields predictions in a good agreement with the field measurements, while hardening soil small strain model gives slightly worst predictions.

KEYWORDS

rigid inclusion-supported embankment, constitutive models, hardening soil, hardening soil model with small-strain stiffness, soft soil creep, finite element modeling

1. INTRODUCTION

Construction of highways and railways on soft soils is considered a challenge for the civil engineers. Embankments over soft soil are possible through many technologies [1], one of these technologies in this field is rigid inclusions. This technology fulfills the intolerable requirements regarding settlements and stability of embankments. Various generations of methods are used to design rigid inclusions under embankments, the first generation includes, for example but not limited to, Hewlett and Randolph [2], Low [3] and Abusharar [4] methods, whereas van Eekelen [5, 6], Zhuang [7], Cui [8] and others proposed different analytical methods in the last decade. None of these methods takes the influence of all parameters into account due to difficulty in creating a comprehensive model and that leads to distinct differences in the design results. To include the influences of all parameters, Finite Element Method (FEM) is considered an adequate method for design to overcome the difficulties of analytical methods. And many FEM programs are currently utilized in the geotechnical field such as Plaxis, Abaqus and Flac.

In spite of the importance of finite element method, however the engineers' encounter many discrepancies between real and numerical models, the sources of these discrepancies are varied (the proper constitutive model, simplifications in geometry, uncertainties of project features, etc.). The comprehension of the discrepancies is fundamental for an appropriate validation of the model. The validation process includes the validation of the model components (constitutive model, input parameters, boundary conditions, etc.) and the validation of integral model through comparing the results of a numerical model and measurements, which can be obtained during the project implementation or from software programs, which use independent solutions [9].

Different constitutive models were proposed to describe the behavior of soil but none of these models can represent the complex behavior of soil under all conditions. Gangakhedkar

*Corresponding author.
E-mail: rashad.seirawan@gmail.com

[10], Bohn [11] and Phutthananon [12], and Ariyarathne [13] suggested Soft Soil (SS) model, Hardening Soil (HS) model, and Modified Cam-Clay (MCC) model, respectively to simulate the behavior of soft soils under embankments supported by rigid inclusions. All these models gave reasonable results in comparison with the field measurements each according to own conditions. Despite that, these models neglect the creep behavior of soft soils, which is characterized by the high compressibility. The Soft Soil Creep (SSC) model was suggested [14] to take the creep into account even if the expected time of this phenomenon exceeds 10 years.

This paper highlights the performance of three constitutive models, i.e., HS, Hardening Soil model with Small-strain Stiffness (HSS), and SSC by using Plaxis 3D Connect Edition V20 program to predict the settlements in subsoil layers, differential settlements, and vertical stresses in the Load Transfer Platform (LTP). A case study of an embankment supported by rigid inclusions and two layers of a geogrid is adopted to perform the comparison between the field measurements and predictions of the advanced models. The objective of this paper is to assist engineers in choosing the suitable constitutive models for similar projects in the numerical analysis.

2. A CASE STUDY OF RIGID INCLUSION-SUPPORTED EMBANKMENT

A railway line connecting two cities in France (Tours and Bordeaux) under the name of the South Atlantic Europe high-speed railway line was constructed, part of this line crosses Virvée swamp. Figure 1 shows a typical geotechnical profile in this region, which is characterized by many layers of soft soils (silty clay, peat and clay) located above a layer of gravel. The levels of soils are associated with an adopted zero level, which is the French georeferenced level (NGF) [15].

To verify the design, a full-scale test of the embankment was constructed, a network of eighty piles and two layers of geogrid were installed to support this embankment. Much instrumentation was installed to measure the settlements and vertical stresses as following (Fig. 2):

		γ (kN/m³)	φ (°)	c (kPa)	OCR
+2.5					
+1.5	Working platform	21.0	35	5.0	–
+0.5	Silty clay	15.0	29	4.0	8.4
±0.0					
-2.0	Peat	10.6	29	4.0	7.85
-4.0	Clay 1	14.0	29	4.0	3.23
-7.5	Clay 2	14.5	29	4.0	1.45
	Gravel	20.0	35	10.0	–

Fig. 1. The soil profile

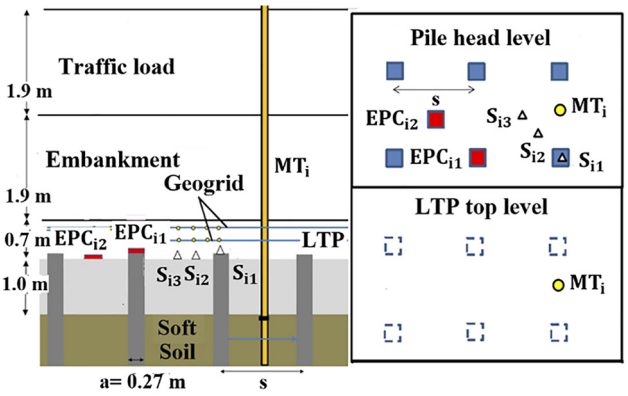

Fig. 2. The instrumentations' locations in the cross-section view (left) and plan view (right)
(*Source:* on the basis of [15])

1. Earth Pressure Cells (EPCs) were fixed inside and over the LTP;
2. Magnetic probe exTensoeter (MT) was placed in the soft soil and six magnet rings were used to measure the settlements in the soft soil layers;
3. Settlement sensors (S_i) were installed to measure the vertical displacement (S_{i1}) of the pile head, and settlements at the two representative measurement points (S_{i2}, S_{i3}) inside the LTP [15].

The working platform was constructed to facilitate the movements of equipment before construction stages. The piles were driven as a first stage of construction, the pile section equal to 0.0751 cm^2 and the pile spacing is $s = 1.6$ m. The LTP with 0.7 m thick was constructed in the second construction stage. This platform includes two layers of uniaxial geogrid (the stiffness $J = 13{,}000$ kN m^{-1}) located 0.2–0.4 m over the pile head level respectively. The last stages include the construction of the embankment with 1.9 m thick and extra part of embankment with 1.9 m thick to simulate the traffic load [15]. The properties of embankment fill, working platform soil and piles and are listed in Table 1.

3. NUMERICAL MODELING OF THE CASE STUDY

Since the analysis of embankment supported by rigid inclusions is a three-dimensional problem, Plaxis 3D program is adopted in this analysis. HS model is utilized to simulate the behavior of the embankment, working platform and gravel soils. Three models are utilized to simulate the soft soils i.e., HS, HSS and SSC, the analysis of these soils is modeled as undrained. The piles are modeled as embedded beam elements and not as elastic linear material due to the convergence problem, which triggered by the interaction between soil and piles and the geogrid is modeled as elastoplastic material.

The piles rows, geogrid layers and finite element mesh in this three-dimensional problem are shown in (Fig. 3). The lengths of the embankment base and surface are 12.0 m, 7.0 m

Table 1. The properties of embankment fill, working platform soil, piles and geogrid

Embankment fill	$\gamma = 21\,\text{kN m}^{-3}$	$\varphi = 35°$	$\Psi = 5°$	$c = 5\,\text{kPa}$	$E_{50} = 16{,}000\,\text{kPa}$	$E_{oed} = 16{,}000\,\text{kPa}$
	$E_{ur} = 48{,}000\,k\text{Pa}$	$m = 0.5$			$k = 0.864\,\text{m day}^{-1}$	
Working platform soil	$\gamma = 21\,\text{kN m}^{-3}$	$\varphi = 35°$	$\Psi = 5°$	$c = 5\,\text{kPa}$	$E_{50} = 12{,}860\,\text{kPa}$	$E_{oed} = 12{,}860\,\text{kPa}$
	$E_{ur} = 38{,}580\,k\text{Pa}$	$m = 0.5$			$k = 0.864\,\text{m day}^{-1}$	
Pile	$\gamma = 24\,\text{kN m}^{-3}$	$E = 20\,\text{GPa}$		$\nu = 0.2$		$L = 12.7\,\text{m}$

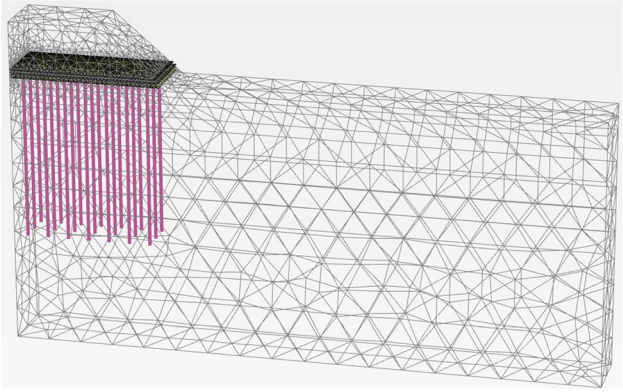

Fig. 3. Finite element mesh of the case study

respectively [15]. The periods and the elevations of the construction stages, and the post-construction period are summarized in Table 2.

3.1. Hardening soil model

HS is used to simulate the behavior of soft and stiff soils. HS model is considered as an extension of Mohr-Coulomb model through using the same failure parameters but it can be characterized by the pre-consolidation stress [16]. Duncan and Chang [17] developed a hyperbolic formulation under a plasticity theory to define the stress-strain relationship.

A pressure-meter test was performed on the site to determine the pressiometric modulus E_M (kN m^{-2}). The analysis by HS model requires calculating the soil stiffnesses based on Eq. (1) and (2) [11].

$$E = E_{oed}\frac{(1+\nu)(1-2\nu)}{(1-\nu)}, \tag{1}$$

$$E_{oed} = E_M/\alpha, \tag{2}$$

where α is a rheological factor and depending on the soil type and consolidation state of the soil [11], E_{oed} (kN m^{-2}) is an oedometric modulus, instead of the Young modulus HS model uses the secant stiffness modulus E_{50} (kN m^{-2}). The following assumption was used for the modeling $E_{50} \approx 2\,E_{oed}$ [14]; ν is a Poisson's ratio and equal to 0.35 for all soft soils.

HS model involves ten well-known input parameters, and theses parameters of the different soils are listed in Table 3.

Table 2. The construction stages

Construction stage	Period (day)	NGF elevation (m)
Working platform	30	+2.5
Pile driving	60	-
Load transfer platform	30	+3.2
Embankment	30	+5.1
Traffic load	30	+7.0
Post-construction	365	-

3.2. Hardening soil model with small-strain stiffness

Benz [18] developed the HS model by taking into account the small strain characteristics of soil. While the HS model requires ten parameters, HSS model requires two additional parameters (the reference shear modulus at small strain G_0^{ref} and the reference strain threshold $\gamma_{0.7}$). These parameters can be obtained by the in-situ tests, the laboratory tests or the correlations with diverse parameters of soil and tests [19].

In this analysis, (G_0^{ref}) is calculated by using Eq. (3)

$$G_0^{ref} = \rho\, V_s^2, \tag{3}$$

where ρ is the soil density, V_s is the shear wave velocity.

In plastic soils, the effect of Over-Consolidation Ratio (OCR) cannot be neglected, based on that, Stokoe [18] suggested Eq. (4) to calculate $(\gamma_{0.7})$ as follows:

$$\gamma_{0.7} = \gamma_{0.7}^{ref} + 5.10^{-6}.I_P.\,OCR^{0.3}, \tag{4}$$

where $\gamma_{0.7}^{ref}$ is the reference shear strain threshold and equal to 1.10^{-4}, I_P is the plasticity index. G_0^{ref} and $\gamma_{0.7}$ values of the different soils are listed in Table 4.

3.3. Soft soil creep model

HS and SS models are used to simulate the behavior of peat, organic and soft soils but these soils are characterized by their high compressibility, wherefore, the SSC model was suggested to take the creep behavior (secondary settlements) into account. Buisman [20] suggested a first law of creep. Many researchers, like Vermeer, Neher and Brinkgreve, [14] worked to develop the creep model depending on the viscoplasticity theory and modified cam clay concept.

The main parameters in the SSC model are, the modified compression index λ^* , the modified swelling index κ^*, the modified creep index μ^*, the internal friction angle φ, the soil cohesion c and the angle of dilation Ψ [14, 21].

In this analysis, the period of monitoring is one year after the end of the construction stages and it is difficult to observe the creep phenomenon. The values of λ^*, κ^* and μ^* of the different soft soils are listed in Table 5.

Table 3. The parameters of the soils for the HS model

Layer	Silty clay	Peat	Clay 1	Clay 2	Gravel
NGF elevation (m)	+1.5	+0.5	−2	−4	−7.5
γ_{unsat} (kN m^{-3})	11.56	6.2	13.0	13.5	19
γ_{sat} (kN m^{-3})	15.0	10.6	14.0	14.5	20
φ°	29	29	29	29	35
Ψ°	0	0	0	0	5
c (kPa)	4	4	4	4	10
E_{50}^{ref} (kN m^{-2})	1,850	800	800	800	63,000
E_{oed}^{ref} (kN m^{-2})	1,850	400	400	400	63,000
E_{ur}^{ref} (kN m^{-2})	5,550	2,400	2,400	2,400	189,000
m	0.65	0.6	0.6	0.6	0.5
K_0^{nc}	0.515	0.515	0.515	0.515	0.426
ν_{ur}	0.2	0.2	0.2	0.2	0.2
R_f	0.9	0.9	0.9	0.9	0.9
k_x, k_y (m day^{-1})	8.64E-4	5.55E-4	6.25E-4	5.55E-4	1.00
k_z (m day^{-1})	8.64E-4	6.75E-4	6.25E-4	5.55E-4	1.00
Over Consolidation Ratio (*OCR*)	8.40	7.85	3.23	1.45	-

Table 4. The additional parameters of the soft soils for the HSS model

Layer	V_s(m/s)	G_0^{ref}(kN m^{-2})	I_P	$\gamma_{0.7}$
Silty clay	60	5504	17	2.60*10^{-4}
Peat	70	5244	53	5.90*10^{-4}
Clay 1	70	6992	34	3.41*10^{-4}
Clay 2	80	9460	38	3.12*10^{-4}

Table 5. The isotropic soft soils parameters of SSC model

Layer	λ^*	κ^*	μ^*
Silty clay	0.0928	0.0232	0.0027
Peat	0.2560	0.0845	0.0010
Clay 1	0.2016	0.0537	0.0019
Clay 2	0.1895	0.0475	0.0018

4. RESULTS AND DISCUSSION

In this section, a comparison is conducted between measured parameters in the field and those predicted by HS, HSS and SSC models based on the back analysis method. The monitoring initiated at the end of the embankment construction stage (+5.1) m NGF and continued 12 months, after the construction stages end.

The measured and predicted settlements under the embankment in various depths (0.5, -1.5, -3.75, -7.25, -10, -11) m NGF at the end of the embankment stage are shown in (Fig. 4 *left*) and at the end of the traffic load stage are shown in (Fig. 4 *right*). HS model yields reasonable values of settlements compared with those obtained from the field measurements, the largest difference does not exceed 10.0 mm. HSS model gives settlements smaller than those measured in the field where the difference reaches 20.0 mm. SSC model predicts satisfying settlement values where the maximum difference with the field observations does not exceed 9.0 mm in these stages, add to that, SSC model considers the creep behavior of these soils.

Likewise (Fig. 5), shows the settlements calculated by HS, HSS, SSC models and those measured in the field, 8 months (*left*) and 12 months (*right*) respectively after the construction period. HS model gives settlement values relatively close to those of the field measurements. Regarding HSS model, the gap between the measured settlements and predicted by using this model expands during the consolidation period. SSC model yields settlements in good agreement with the field measurements, the SSC-predicted settlements are considered the most satisfying in comparison with those of other models. One exception can be noticed in the point located at the depth -1.5 m where the prediction of HS model is better than that of SSC model by approximately 3.0 mm. The largest differences between predicted settlements by using SSC and HS models with measured settlements are approximately (13.0, 16.0) mm respectively while HSS model gives relatively unacceptable results.

Figure 6 demonstrates a comparison between the measured and predicted vertical stresses at the pile head and embankment base levels, the stress is concentrated at the pile head as a result of the soil arching phenomenon. HS model yields close stresses to those measured by the EPC_{i1} during the various stages of construction, and post-construction period, while the stresses calculated by HSS model are relatively low. SSC model gives slightly larger stresses than the measurements, the final values of the stresses at the end of the monitoring period are as following, (σ_{meas} = 2,650 kPa, $\sigma_{HS,calc}$ = 2,630 kPa, $\sigma_{HSS,calc}$ = 2,421 kPa, $\sigma_{SSC,calc}$ = 2,780 kPa).

In respect of the stresses measured by the EPC_{i2}, SSC model provides the best predictions. The low values of stresses in this point are associated with soil arching phenomenon and tension forces in the geogrid layers (see Fig. 6).

Figure 7 shows the differential settlements between the selected measurement points (S_{i2}, S_{i3}) located on the

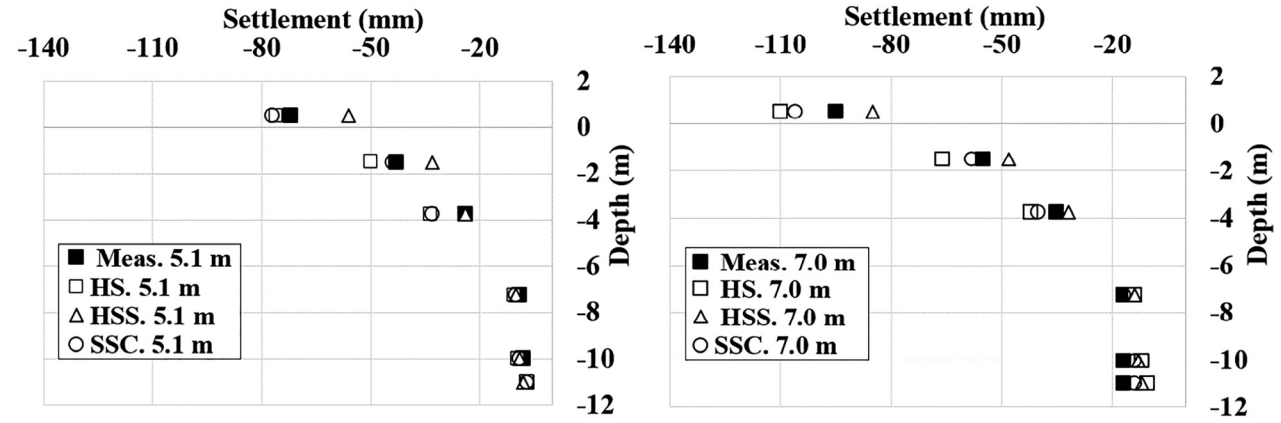

Fig. 4. Settlements at the end of the embankment construction stage (left) and traffic load stage (right)

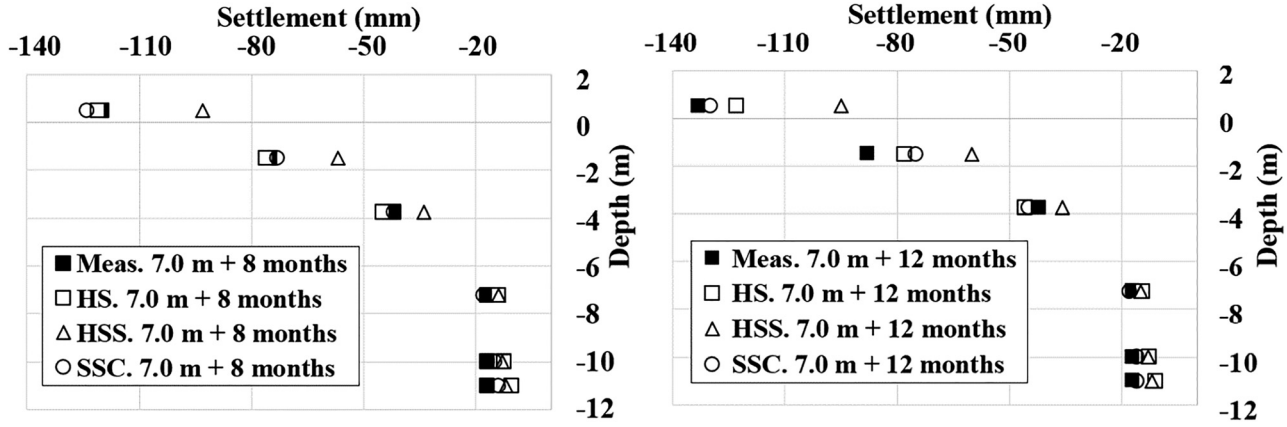

Fig. 5. Settlements under the embankment after 8 months (left) and 12 months (right)

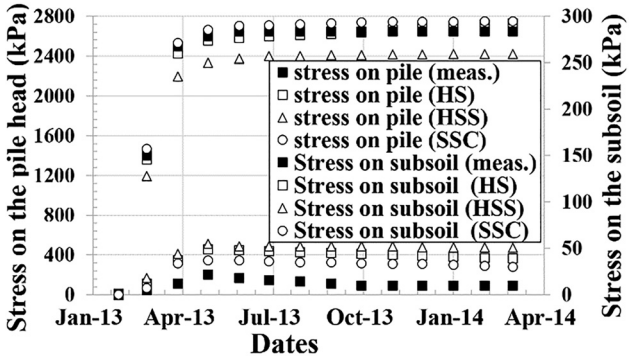

Fig. 6. Vertical stresses at the pile head and embankment base levels

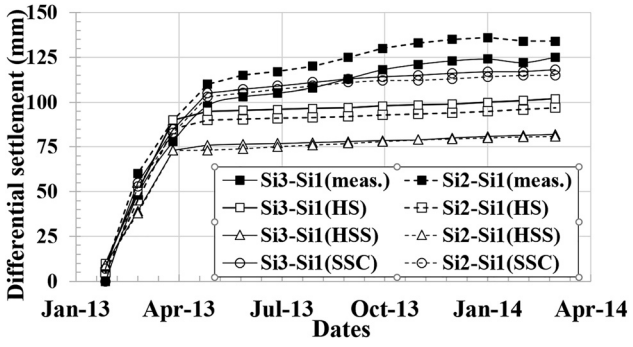

Fig. 7. Differential settlements between the pile head (S_{i1}) and points (S_{i2}, S_{i3})

embankment base and selected point (S_{i1}) located on the pile head. The HS model gives values of differential settlements smaller than those obtained from the field measurements, the difference between measured and predicted differential settlements is approximately 24% at the end of monitoring period. HSS model results are less than those calculated by HS model and much smaller than the measurements. SSC model predicts the differential settlements relatively well; the largest difference between the final values is approximately 14%. This discussion leads to accept SSC model as the suitable model to solve this type of problems due to the convergence between the results and consideration of the creep behavior of the soft soil.

5. CONCLUSION

The paper demonstrates a comparison between three advanced constitutive models, i.e., HS, HSS and SSC to simulate the soil layers for evaluating their performances in

predicting settlements and stresses. The conclusions of this study are as following:

- HS model yields reasonable settlements at the end of construction stages and consolidation stages with the largest difference do not exceed 10.0 and 16.0 mm, respectively. The vertical stresses are relatively close to the field measurements at the end of monitoring period, on the pile head, the vertical stresses are as following σ_{meas} = 2,650 kPa, $\sigma_{HS,calc}$ = 2,630 kPa. The differential settlements calculated by HS model are underestimated by approximately 24%;
- The reference shear modulus at small strain G_0^{ref} and the reference strain threshold $\gamma_{0.7}$ are calculated by Eqs (3) and (4) in this case study. The values of settlements and vertical stresses are much smaller than the field measurements, the maximum difference between measured and calculated settlements is about 40 mm while with the differential settlements is about 55 mm;
- With the SSC model, the predicted settlements are generally very close to the field measurements at the end of the construction stages and the consolidation period. It is observed that the largest difference does not exceed 9.0 and 13.0 mm, respectively. The vertical stresses are slightly larger than the field measurements and the stresses on the pile head σ_{meas} = 2,650 kPa, $\sigma_{SSC,calc}$ = 2,780 kPa. SSC model gives predictions of the differential settlements in a good agreement with the field measurements; the difference is around 14% which is considered reasonable.

REFERENCES

[1] E. Koch, "Monitoring of embankment construction processes," *Pollack Period.,* vol. 2, no. 1, pp. 89–100, 2007.

[2] W. J. Hewlett and M. F. Randolph, "Analysis of piled embankments," *Ground Eng.*, vol. 22, no. 3, pp. 12–18, 1988.

[3] B. K. Low, S. K. Tang, and V. Choa, "Arching in piled embankments," *Geotechnical Eng.*, vol. 120, no. 11, pp. 1917–1938, 1994.

[4] S. W. Abusharar, J. J. Zheng, B. G. Chen, and J. H. Yin, "A simplified method for analysis of a piled embankment reinforced with geosynthetics," *Geotextiles Geomembranes*, vol. 27, no. 1, pp. 39–52, 2008.

[5] S. J. M. Van Eekelen, A. Bezuijen, H. J. Lodder, and A. F. van Tol, "Model experiments on piled embankments," Part I, *Geotextiles and Geomembranes*, vol. 32, pp. 69–81, 2012.

[6] S. J. M. Van Eekelen, A. Bezuijen, H. J. Lodder, and A. F. van Tol, "Model experiments on piled embankments," Part II, *Geotextiles and Geomembranes*, vol. 32, pp. 82–94, 2012.

[7] Y. Zhuang, X. Cheng, and K. Wang, "Analytical solution for geogrid-reinforced piled embankments under traffic loads," *Geosynthetics Int.*, vol. 27, no. 3, pp. 249–260, 2020.

[8] X. Cui, Y. Zhuang, S. Ning, and K. Wang, "An analytical method to calculate the settlement of reinforced piled embankment considering three-dimensional deformed geogrid," *Eur. J. Environ. Civil Eng.*, 2020, https://doi.org/10.1080/19648189.2020.1810130.

[9] R. B. J. Brinkgreve, "Validating geotechnical finite element models," *3rd Inter. Symposium on Computational Geomechanics*, Krakow, Poland, August 21–23, 2013, pp. 292–304.

[10] R. Gangakhedkar, "Geosynthetic reinforced pile supported embankments," MSc Thesis, University of Florida, 2004.

[11] C. Bohn, "Serviceability and safety in the design of rigid inclusions and combined pile-raft foundations," PhD Thesis, Paris-Est University, 2015.

[12] C. Phutthananon, P. Jongpradist, and P. Jamsawang, "Influence of cap size and strength on settlements of TDM-piled embankments over soft ground," *Mar. Georesources Geotechnology*, vol. 28, no. 6, pp. 686–705, 2019.

[13] P. Ariyarathne and D. S. Liyanapathirana, "Review of existing design methods for geosynthetic-reinforced pile-supported embankments," *Soils and Foundations,* vol. 55, no. 1, pp. 17–34, 2015.

[14] R. B. J. Brinkgreve, L. M. Zampich, and N. Ragi Manoj, *Plaxis Connect Edition V20.* Delft University of Technology & Plaxis B, The Netherlands, 2019.

[15] L. Briançon and B. Simon, "Pile-supported embankment over soft soil for a high-speed line," *Geosynthetics Int.*, vol. 24, no. 3, pp. 293–305, 2017.

[16] P. G. Bonnier, P. A. Vermeer, and T. Schanz, "Formulation and verification of the Hardening-Soil model," *Proceedings on Beyond 2000 Coput. Geortechnics*, Routledge, Amsterdam, 1999, pp. 1–10.

[17] J. M. Duncan and C. Y. Chang, "Nonlinear analysis of stress and strain in soils," *J. Soil Mech. Found. Division*, vol. 96, no. 5, pp. 1629–1653, 1970.

[18] T. Benz, "Small-strain stiffness of soils and its numerical consequences," PhD Thesis, University of Stuttgart, 2007.

[19] Z. Rémai, "Settlement below embankments: factors controlling the depth of the deformation zone," *Cent. Eur. Geology.*, vol. 57, no. 1, pp. 71–81, 2014.

[20] A. S. K. Buisman, "Results of long duration settlement observations," in *Proceedings of the 1st International Conference of the ISSMFE*, Cambridge, UK, June 22–26, 1936, pp. 103–106.

[21] E. Koch, "Input parameters of Transdanubian clay for the hardening soil and soft soil models," *Pollack Period.*, vol. 4, no. 1, pp. 93–104, 2009.